EXPERIMENTAL STUDY OF THE FLOW IN A SIMULATED HARD DISK DRIVE

Charlotte Barbier, Joseph A. C. Humphrey and Eric Maslen
Department of Mechanical and Aerospace Engineering
University of Virginia
Charlottesville, VA 22904, USA
cb2ps@virginia.edu, jach@virginia.edu, ehm7s@virginia.edu

ABSTRACT

Instantaneous circumferential and radial velocity components of the air flowing past a symmetrical pair of suspension/slider-units (SSUs) attached to an E-Block/arm were measured in an especially designed corotating disk apparatus using the particle image velocimetry technique. The geometrical components in the apparatus test section are scaled by a factor of two relative to those of a nominal 3½ inch hard disk drive. Most of the measurements were obtained on the interdisk midplane for two angular orientations of the SSUs: one with the tip of the SSUs near to the hub supporting the disks, and one with the tip of the SSUs near the rims of the disks. Data obtained at 250, 500, 1000, 1500 and 2000 rpm were post-processed to yield mean and rms values of the two velocity components, the mean axial vorticity, and the turbulent kinetic energy (based on the two velocity components). By 2000 rpm the mean velocity components were asymptotically independent of disk speed of rotation but their rms values appeared to still be evolving. Aside from their intrinsic fundamental value, discussed in the text, the data serve to guide and test the development of numerical procedures for predicting this complex class of enclosed rotating flows.

THE PROBLEM OF INTEREST

Background and Prior Work

Increasingly, the trend in the computer disk drive industry is to manufacture smaller hard disk drives (HDD) with disks rotating at relatively high rpm. The trend is driven by the desire to miniaturize drives for hand-held devices and other small-scale applications while maintaining high rates of electronic information transfer. The trend has been facilitated by major advances in the areas of electromagnetic recording materials and technologies that allow for very high information storage densities (INSIC, 2004). The disks in current nominal 3½ inch drives typically have information densities of 100K tracks per inch (TPI) and rotate between 4,200 and 15,000 rpm. Future 1 inch drives are expected to have information densities upwards of 35K TPI and to rotate between 3600 and 5400 rpm. The combination of high track densities, small geometrical dimensions, and high speeds of rotation of the disks contribute to the problem of magnetic head positioning error and associated track misregistration due to flow-induced vibrations. As a consequence, there is a need to better understand and render predictable the flow-structure interactions arising in these devices.

The unobstructed flow in the space between a pair of disks corotating at high rpm in a cylindrical enclosure has been the subject of considerable research. Measurements by Abrahamson et al., 1989 and Humphrey and Gor, 1993, and calculations by Schuler et al., 1990 and Humphrey et al., 1995 reveal a pair of toroidally-shaped counter-rotating vortices in the interdisk space that are induced by the centrifugally-driven flow arising in the thin Ekman layers on the disk surfaces. A circumferential instability corrugates these vortices to create circumferentially distributed foci of the axial component of vorticity that rotate at about 75% - 80% of the disk angular velocity. Nearer the hub connecting the disks the interdisk flow approaches solid body rotation. However, because of the shearing action by the enclosure wall, the flow near the rims of the disks transitions to the turbulent regime with increasing disk angular velocity and is convected radially inwards along the interdisk midplane by the pressure field force that balances the centrifugal force.

In contrast to the unobstructed flow case, relatively little information exists in the archive literature pertaining to the obstructed flow. Exceptions are the experimental studies by Abrahamson et al. (1991), Tzeng and Humphrey (1991), Humphrey et al. (1992), Usry et al. (1993), Gross (2003) and the analytical and numerical investigations of Suzuki and Humphrey (1997), Shimizu et al. (2001, 2003), Kubotera et al. (2002), Tsuda et al. (2003), Humphrey et al. (2003), Kazemi (2005). The experimental studies are mainly focused on the effects of a single, relatively large obstruction in the space between the disks that is meant to simulate the effects of an actuator arm on the flow. However, such a geometry alone fails to capture the effects of the SSUs attached to it, or of the flow-mediated interactions that arise between the SSUs and the arm. Notwithstanding, these studies show that, depending on its relative angular orientation: (i) the flow approaching a simulated actuator arm can accelerate significantly in the interdisk space as a consequence of the partial blockage the arm creates; (ii) the flow is strongly sheared with the possible formation of vortical structures at the tip of the arm where it connects to the SSUs.

The numerical studies present more detailed impressions of the flows around the actuator arm and the SSUs attached to it. The LES flow calculations by Shimizu et al. (2001, 2003) suggest that the following contribute to SSU vibrations: (i) pressure fluctuations in the space between a pair of SSUs, and in the flow that is ingested from the enclosure surroundings back into the interdisk space downstream of the SSUs; (ii) for suspensions of U-shaped cross-section, discrete mode high-frequency vortex shedding from the suspension flange for an inner tracking SSU orientation, and multimode low-frequency vortex shedding from the arm for an outer tracking orientation. Tsuda et al. (2003) have performed DNS calculations of the flow past an actuator arm with and without a weight-saving hole in it. For both cases, a 3D spiral vortex arises downstream of the arm that affects arm vibrations. However, the characteristics of the spiral flow and associated arm vibrations are also affected by the flow generated in and spilling from the hole when present. Limited laser-Doppler velocimetry and vibrometry data are presented in support of the numerical findings. While very valuable, the computational time and storage requirements of calculation based approaches limits numerical studies to relatively specific geometrical and dynamical conditions, thus precluding systematic investigations of the effects of relevant parameters on the flow past arms and SSUs and of the attendant flow-induced SSU vibrations.

Because of the major challenges associated with measuring and calculating this class of highly unsteady 3D flows and the SSU vibrations they induce, the problem has been investigated numerically by reference to simpler and much more computationally affordable 2D approximations of the unsteady flow fields; see Humphrey (2002) and the references therein. This approach allows an improved qualitative understanding of the physics underpinning flow-induced SSU vibrations. However, because the component of motion tangent to the arm and the SSUs attached to it is significantly larger than the normal component (Humphrey, 2003), and because of the geometrical variations, including weight-saving holes, that arise in the tangential direction, the 2D flow approach is limited in its ability to guide design improvements essential for minimizing SSU vibrations.

Relevant Considerations

We are concerned with quantifying the properties of the flow of air in a simulated HDD with focus on fluid motion in the vicinity of the E-block/arm/SSUs. A characteristic Reynolds number of the flow between a pair of corotating disks in a HDD may be defined as $Re_H = \Omega R_d H/\nu$; where Ω (rad/s) is the angular velocity of the disks, R_d (m) is the radius of the disks, H (m) is the spacing between the disks and ν (m^2/s) is the kinematic viscosity of air. For current 3½ inch drives with $H \approx 2$ mm, the range in Re_H is 2,250 - 9,500, while for 1 inch drives with $H \approx 0.6$ mm it is likely to be 200 – 300, approximately. At these Reynolds numbers for the 3½ inch drives, the flow in the vicinity of the disk rims and past the arm and SSUs is turbulent while that nearer the hub is much less so. However, because of the geometrical scales of various objects in the path of the flow, Re_H alone does not inform unambiguously on the nature of the fluid motion and, at a minimum, it is necessary to also consider the geometry and angular orientation of the E-block, arm and SSUs in the interdisk space.

The suspension of a SSU is tapered, being wide at its base where it connects to the supporting arm, and narrow at its tip where the slider supporting the read/write magnetic head is located. The cross-section of a suspension can be rectangular or U-shaped. Like the arm, the suspension may have weight-saving holes punched in it. Combined, the E-block, arm and SSUs block and redirect a significant part of the interdisk flow approaching these units. As a consequence, one expects significant flow-structure interactions, partly as the result of highly vortical motions in the wakes of the arm, the suspensions, and the sliders attached to the suspension tips. The extent of these interactions depends on the relative angular orientation of these objects with respect to the approaching flow. With reference to Fig. 1, for one case, the ‘inner configuration’ (IC), the tip of a SSU is located closer to the hub to which the rotating disks are attached. For the other case, the ‘outer configuration’ (OC), the tip is located closer to the rim of the rotating disk on which the slider flies. In the IC case, the arm and SSUs present the largest cross-section projection to the approaching flow, favoring strong flow-structure interactions in spite of the solid body rotation nature of the flow nearer the hub. In the OC case, even though the arm and SSUs are more closely aligned with the approaching flow, the slider at the tip of the SSU is immersed in a region of very high rotational velocity, where the largest levels of turbulence are induced by shearing of the flow by the fixed enclosure wall.

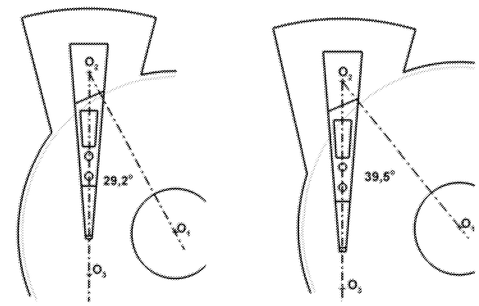

Fig. 1. Plan view of a section of the test section showing to the left the inner (IC) and to the right the outer (OC) E-block/arm/SSUs configurations investigated. The E-block fits into a cavity on the side of the enclosure. The hub and disks rotate counter-clockwise.

THE EXPERIMENT

Apparatus

Sketches of the corotating disks flow apparatus and of the E-block/arm/SSUs assembly investigated are provided in Fig. 2. To facilitate optical accessibility to the flow, all essential geometrical dimensions in the test section were scaled by a factor of 2 relative to a 3½ HDD. Two enclosures were built of plexiglass, one for the IC and another for the OC configurations investigated. The E-block fits into a cavity on the side of the enclosure and the arm/SSUs penetrate the interdisk space symmetrically with respect to the interdisk midplane. Of the two disks in the test section, the bottom is made of anodized aluminum and the top of glass. Both disks have a radius of 10 cm and a thickness of 2mm. Their surfaces are flat (< 6.4 μm) and optically smooth. The disks are spaced 4.8 mm apart by a solid anodized aluminum ring of outer radius 2.86 cm, and the spacing between the rims of the disks and the inner wall of the enclosure is 3 mm. Disk wobble is estimated to be less than 125 μm and of no consequence to the flow established in the interdisk space. The disks are clamped down about a spindle that is driven by a brushless DC electric motor with a speed range of 10 to 5000 rpm. The motor is fixed to the inside of a massive hollow metal cylinder such that the apparatus is essentially vibration free for the rotational speeds investigated. A shaft encoder for feedback control of rotor speed is mounted to the motor and its signal is provided to a GALIL DMC 1417 motion control board.

Equipment

A TSI Power View system was used to perform the PIV measurements. This system employs a pair of New Wave Solo Dual Nd:YAG lasers (50 mJ/pulse, 532 nm wavelength). An articulated arm with an optical head attached, consisting of a 200 mm spherical lens combined with a –15 mm cylindrical lens is used to produce a laser light sheet 46 mm wide, and 0.04 mm at the waist with a divergence angle of 0.017 rad (1.75mm/100mm).

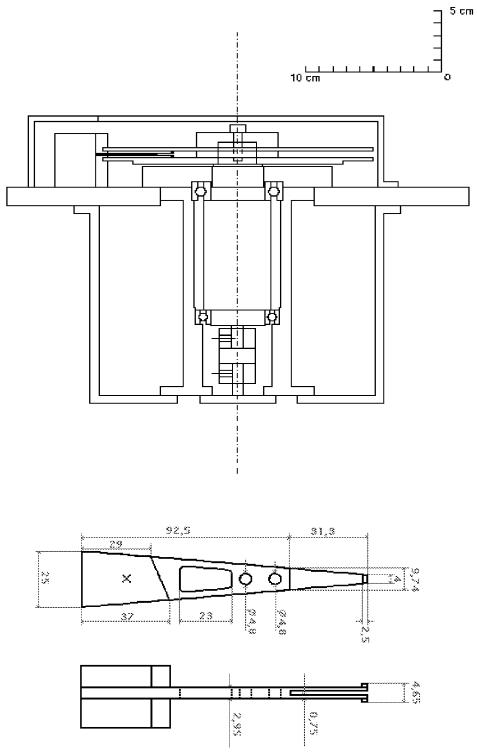

Fig. 2. Sketches and dimensions of corotating disks flow apparatus (top, cm: side view) and of the E-block, arm and SSUs in the test section (bottom, mm: plan and side views). Note weight-saving holes punched in the arm between the E-block (left) and SSUs (right). The two angular orientations of the E-block/arm/SSUs investigated in the test section are shown in Fig. 1.

The duration of a single laser pulse is 3-5 ns and the time between pulses ranges between 80 μs at low fluid velocities and 10 μs at high velocities. A Power View 4M CCD camera with an AF Nikkor (Nikon) 60 mm f2.8 lens set at about 18 cm from the enclosure is used to capture the PIV images. The camera has 2K x 2K pixel resolution (12-bit digital output) at 17 frames/s. The system is controlled by a Laser Pulse Computer Controller Synchronizer interfaced to a Dual Processor Intel Xeon 2.0 GHz PC computer with 1 GB RAM and with a total storage of 400 GB. TSI Insight 4 software is used for image acquisition and subsequent post-processing. Two-frame cross-correlations were performed on 300 image pairs by means of FFT using a Gaussian peak search algorithm. In a single acquisition of two consecutive images, a procedure utilizing velocity cutoff limits and a local mean filter is applied for removing spurious data. Flow statistics (mean and rms values of the circumferential and radial velocity components, mean axial vorticity, and the turbulent kinetic energy based on the two velocity components) were derived from the 300 image pairs obtained for each measurement case. A 530 Dell workstation was used to control apparatus motor rotation and the PIV velocity measurements, and to conduct post-processing of the image pairs from which the flow field data were obtained.

To guarantee high quality PIV measurements, the particle seeding agent must be sufficiently dense and homogeneously distributed to have at least 15 particles per interrogation spot (Keane and Adrian, 1990). This is easily achieved by using an interrogation window of 32 pixels. For a 2048 × 2048 pixel image, processed with 50% subregion overlap, a 128 × 128 grid of vectors is obtained with a resolution of 0.428 × 0.428 mm^2. This picture characterizes the flow in a square 54.78 × 54.78 mm^2, which is only a subsection of the total area of interest. The flow field of the entire area of interest is a composite of 6-7 subsections patched together.

A sharper definition of fluid motion near the hub and the E-block/arm/SSUs is obtained by applying fluorescent paint to their surfaces. The fluorescent paint shifts the wavelength of the background light reflected from these surfaces so that, using an appropriate filter, only the light scattered from the seeding agent is detected by the camera. In this way measurements are obtained to within 1-2 mm from these surfaces.

Methodology

Prior to taking a series of PIV measurements, the rotational speed of the disks is fixed. The cavity on the side of the enclosure (Fig. 1) is then flooded with droplets composed of 10% by volume of glycerol in water ($\rho_p \cong$ 1.021 g/cm^3, $d_p \cong$ 1μm) generated by a six jet TSI atomizer. Within about 5 s, after which the measurements are made, the seeding agent has fully dispersed and any flow perturbations associated with particle injection have disappeared. The PIV velocity measurements are made in the interdisk midplane, which passes midway between the two suspensions on the E-block arm. For this, 300 image pairs are taken in groups of 30 image pairs, with the fresh injection of particles taking place between groups. In this way, a series of runs at increasing disk rpm is performed.

Uncertainties

All linear and angular dimensions in the test section are known to better than ± 0.1 mm and ± 1°, respectively. The uncertainty in disk angular velocity is estimated to be less than ± 0.5%. Sources and magnitudes of uncertainties affecting PIV measurements are well documented in the literature (Raffel et al., 1998). We comment here on those relevant to this work. The theoretical (Stokes drag-based) relaxation time of the seeding agent particles ($\tau_p = \rho_p d_p^2/18\mu$) in air at 23 °C is $\tau_p < 3.1$ μs. Since this time scale is two orders of magnitude smaller than the smallest significant time scale associated with energetic eddies in the flow (about 200 μs at 2000 rpm, based on the space between the disks and 10% of the disk rim velocity), particle lag is assumed to be negligible. Although there are no significant optical uncertainties due to the curvature of the enclosure wall, it is critical to align the pulsed laser sheet to illuminate the interdisk midplane. Uncertainties due to out-of-plane particle displacement in an interrogation subregion and to the time between laser pulses are negligible. Assuming a normal distribution for the mean velocity components yields a statistical uncertainty on these quantitires ranging from ± 0.5 to ± 3.5% with 95% confidence. Likewise, assuming a chi-square distribution for the variances yields an uncertainty for the velocity component rms values less than ± 8.7%, also with 95% confidence.

RESULTS AND DISCUSSION

Asymptotic Invariance of the Flow

Velocity component measurements were obtained for 250, 500, 1000, 1500 and 2000 rpm corresponding to a range in Re_H of 800 to 6700. (Note that 2000 rpm in the apparatus corresponds to 10,100 rpm in a 3½ HDD.) The asymptotic

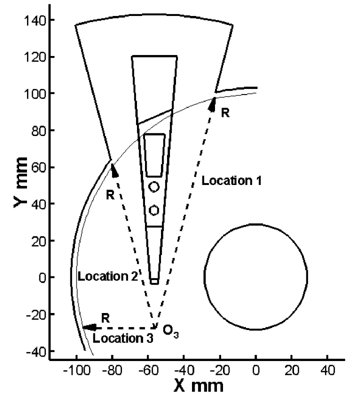

Fig. 3. Locations 1, 2 and 3 where asymptotic invariance of flow is checked.

invariance of the flow was checked by reference to velocity component profiles obtained from the PIV measurements at the locations shown in Fig. 3, upstream and downstream of the E-block/arm/SSUs. Results obtained for the IC configuration of Fig. 1 are shown in Fig. 4. (Note that: i) In all figures, mean and rms velocities are normalized by the rim speed of the disks, ΩR_d; ii) The velocity components in Fig. 4 are plotted relative to an (r, θ) cylindrical coordinate system centered at point O_3. This choice of components facilitates comparisons with 3D DNS calculations being performed on a (r, θ, z) sector centered at point O_3.) It is clear that the means of both velocity components tend to an asymptotic limit with increasing rpm but that the rms values are still evolving. Checks are currently under way to determine whether the rpm of the flow needs to be increased further to achieve a statistically stationary asymptotic state in its turbulent properties, or the sample size (300 image pairs) needs to be increased to more precisely determine the rms velocities. Particularly noteworthy in these plots are: i) the relatively high values of the mean and rms circumferential velocities near the rims of the disks (R ≥ 120 mm along Location 1); ii) the pronounced effect of the sliders at the tip of the suspensions which significantly reduce the speed of the mean flow while markedly increasing its rms (R ≈ 20-40 mm along Locations 1 and 2); iii) the significant reduction in circumferential velocity everywhere at Location 2; iv) the effects of the weight-saving holes on both rms velocities (R ≈ 50-100 mm along Location 2).

Velocity Magnitude and Streamlines, Vorticity and Turbulent Kinetic Energy

Plots of velocity magnitude with streamlines superimposed are shown in Fig. 5 for the IC and OC configurations at 2000 rpm. In both cases, the flow approaching the E-block/arm/SSUs splits in two where the arm attaches to the block, the bulk of the air being redirected and accelerated along the upstream surfaces of the arm and SSUs. However, as mentioned in relation to Fig. 4, the sliders on the SSUs significantly decelerate the flow going past them. The same observations apply to the OC case, except that in this case the region of 3D flow reversal observed near the hub in the IC case is absent. This reversal of fluid motion is due to the larger blockage of the flow in the IC case (56%) relative to the OC (48%) and also occurs at 500, 1000 and 1500 rpm. It has been calculated numerically by Suzuki and Humphrey (1997) for a single, radially aligned, arm-like blockage in the space between a pair of disks corotating in a cylindrical enclosure at 300 rpm.

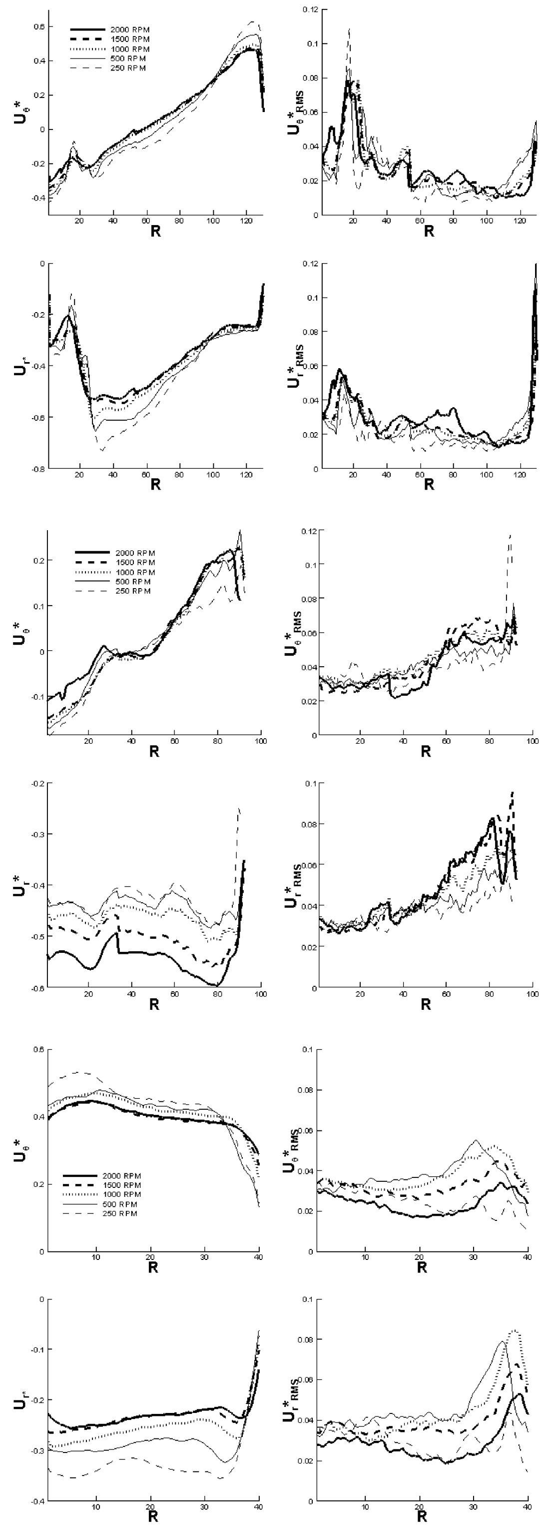

Fig. 4. Mean and rms values of the velocity components as a function of disk rpm at Locations 1 (top) 2 (middle) and 3 (bottom) in Fig. 3. The data are for the IC configuration of Fig. 1.

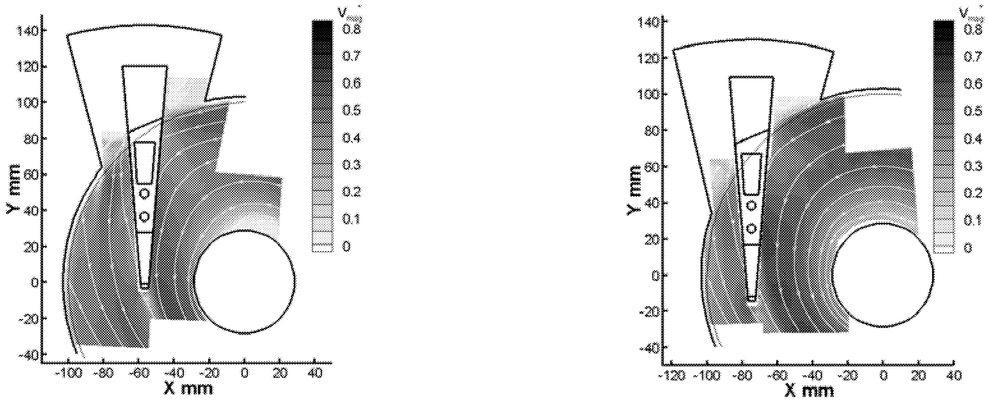

Fig. 5. Mean velocity magnitude contours with streamlines superimposed for IC (left) and OC (right) configurations at 2000 rpm.

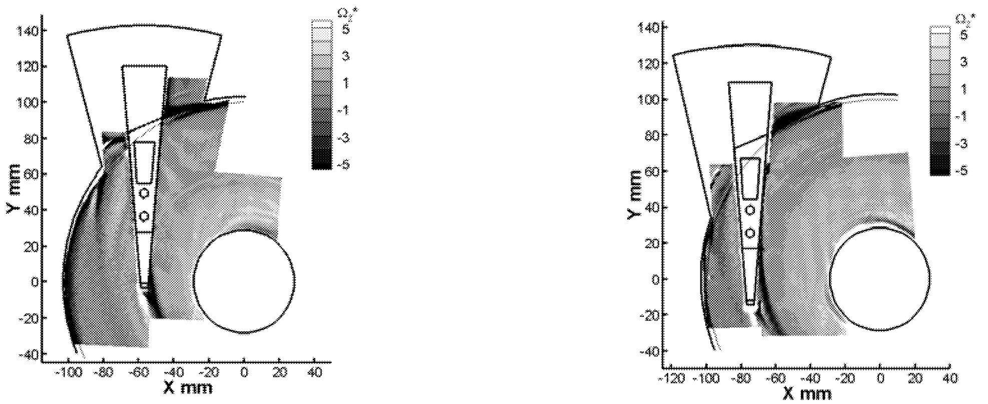

Fig. 6. Mean axial component of vorticity (normal to disk surface) for IC (left) and OC (right) configurations at 2000 rpm.

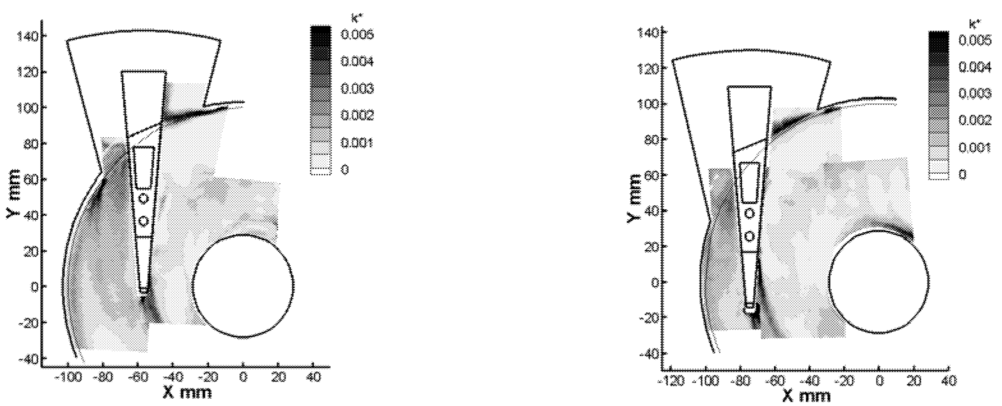

Fig. 7. Turbulent kinetic energy (based on two velocity components) for IC (left) and OC (right) configurations at 2000 rpm.

Corresponding plots for the axial component of vorticity (normal to the disk surface) and the turbulent kinetic energy, $k^* = 1/2(U_{r\,rms}{}^2 + U_{\theta\,rms}{}^2)/(\Omega R_d)^2$, are provided in Figs. 6 and 7. For both the IC and OC case, a strongly vortical and energetic shear layer detaches from the upstream corner of the cavity with the E-block and impinges at the point where the arm connects to the E-block. For the IC case, a second shear layer is formed at the downstream corner of the cavity. Also for both cases, a vortical flow appears in the wake of the sliders on the SSUs, and (more noticeably for the OC case) a curved shear layer is formed on the upstream side of the suspensions that appears to originate at the point where the suspensions attach to the arm.

CONCLUSIONS

Detailed measurements were made for the flow in a simulated hard disk drive that retains the essential physics of a real device. PIV data for two velocity components are presented for a geometrical configuration scaled by a factor of 2, approximately, relative to a 3½ inch HDD. The measurements were made on the interdisk midplane in the presence of an E-block/arm/SSUs assembly, with the arm and SSUs obstructing the interdisk space at two different orientation angles. The highest disk speed of rotation investigated was 2000 rpm, corresponding to 10,100 rpm in a 3½ inch HDD. At 2000 rpm in the experiment, the velocity component means had essentially reached an asymptotically invariant state but the rms velocities appeared to still be evolving.

The data reveal strong influences of the arm and SSUs on the flow that depend on the relative orientation angle of the arm/SSUs in the interdisk space. The blockage presented by these obstructions redirects a large portion of the flow tangentially along the upstream surfaces of the arm and SSUs. Highly vortical shear layers are formed on these surfaces and downstream of the sliders attached to the suspensions. Shear layers also originate at the upstream and downstream corners of the cavity extension to the enclosure. For the IC configuration, a region of 3D flow reversal is observed near the hub surface, upstream of the arm/SSUs.

These results point to a number of sources potentially capable of driving flow-induced SSU vibrations. In this regard, power spectral densities obtained at discrete locations along the length of the arm/SSUs using a hot-wire (not shown here) reveal energetic components of motion between 10 and 500 Hz, especially at the locations where the arm and sliders respectively connect to the SSUs.

A parallel investigation is under way wherein the data from this study are being used to guide and test DNS calculations of the flow configuration, to then predict SSU vibrations using an ANSYS-based FE code.

ACKNOWLEDGEMENTS

The authors gratefully acknowledge financial support provided by INSIC, San Diego, CA, and helpful technical discussions with R. Evans and A. H. Sacks, and the assistance of E. Spenceley, L. Steva, B. Thiede and C. Pfister in designing and constructing the apparatus.

REFERENCES

Abrahamson, S.D., Eaton, J.E. and Koga, D., 1989, "The flow between shrouded corotating disks," *Phys. Fluids A,* Vol. 1, pp. 241-251.

Abrahamson, S.D., Chiang, C. and Eaton, J.K., 1991, "Flow structure in head-disk assemblies and implications for design," *Adv. Info. Stor. Syst.,* Vol. 1, pp. 79-110.

Gross, H.M., 2003, "Off-track vibrations of the read-write heads in hard disk drives," Ph.D. Thesis, University of California.

Humphrey, J.A.C., Schuler, C.A. and Iglesias, I., 1992, "Analysis of viscous dissipation in disk storage systems and similar flow configurations," *Phys. Fluids A,* Vol. 4, pp. 1415-1427.

Humphrey, J.A.C. and Gor, D., 1993, "Experimental observation of an unsteady detached shear layer in enclosed corotating disk flow," *Phys. Fluids A,* Vol. 5, pp. 2438-2442.

Humphrey, J.A.C., Schuler, C.A. and Webster, D.R., 1995, "Unsteady laminar flow between a pair of disks corotating in a fixed cylindrical enclosure," *Phys. Fluids,* Vol. 7, pp. 1225-1240.

Humphrey, J.A.C., Haj-Hariri, H., Iwasaki, T., Kazemi, M. and Rosales, L., 2002, "Modeling and controlling flow-induced suspension-head unit vibrations in hard disk drives," *Microsystem Technologies,* Vol. 8, pp. 375-382.

Humphrey, J.A.C., Kazemi, M. and Herrero, J., 2003, "Method for calculating the velocity of air flowing past a pair of suspensions in a disk drive," *Microsystem Technologies*, Vol. 9, pp. 534-540.

INSIC (Information Storage Industry Consortium), 2004, "The future of storage applications, information continuity from backup to archive," July 18-22, 2004, Monterey, CA.

Kazemi, M.R., 2005, "Numerical modeling of magnetic head positioning rrror due to flow-suspension interactions in disk drives," Ph. D. Thesis, University of Virginia

Keane, R.D. and Adrian, R.J., 1990, "Optimization of particle image velocimeters. Part I: Double pulsed systems," *Meas. Sci. Techn.*, Vol. 1, pp. 1202-1215.

Kubotera, H., Tsuda, N., Tatewaki, M. and Maruyama, T., 2002, "Aerodynamic vibration mechanism of HDD arms predicted by unsteady numerical simulations," *IEEE Trans. Magn.*, Vol. 38, pp. 2201-2203.

Raffel, M., Willert, C. and Kompenhans, J., 1998, "Particle Image Velocimetry – A Practical Guide," Springer-Verlag, Berlin.

Schuler, C., Usry, W., Weber, B., Humphrey, J.A.C. and Greif, R., 1990, "On the flow in the unobstructed space between shrouded corotating disks," *Phys. Fluids A,* Vol. 2, pp. 1760-1770.

Shimizu, H., Tokuyama, M., Imai, M., Nakamura, S. and Sakai, K., 2001, "Study of aerodynamic characteristics in hard disk drives by numerical simulation," *IEEE Trans. Magn.*, Vol. 37, pp. 831-836.

Shimizu, H., Shimizu, T., Tokuyama, M., Masuda, H. and Nakamura, S., 2003, "Numerical simulation of positioning error caused by air-flow-induced vibration of head gimbals assembly in hard disk drive," *IEEE Trans. Magn.*, Vol. 39, pp. 806-811.

Suzuki, H. and Humphrey, J.A.C., 1997, "Flow past large obstructions between corotating disks in fixed cylindrical enclosures," *J. Fluids Eng*., Vol.119, pp. 499-505.

Tsuda N, Kubotera, H., Tatewaki, M., Noda, S., Hashiguchi, M. and Maruyama, T., 2003, "Unsteady analysis and experimental verification of the aerodynamic vibration mechanism of HDD arms," *IEEE Trans. Magn.*, Vol. 39, pp. 819-825.

Tzeng, H. and Humphrey, J.A.C., 1991, "Corotating disk flow in an axisymmetric enclosure with and without a bluff body," *Int. J. Heat and Fluid Flow*, Vol. 12, pp. 194-201.

Usry, W., Humphrey, J.A.C. and Greif, R., 1993, "Unsteady flow in the obstructed space between disks corotating in a cylindrical enclosure," *J. Fluids Eng*., Vol. 115, pp. 620-626.